JACS
JOURNAL OF THE AMERICAN CHEMICAL SOCIETY
Article
pubs.acs.org/JACS

Investigating the α-Effect in Gas-Phase S_N2 Reactions of Microsolvated Anions

Ditte L. Thomsen,[†,‡] Jennifer N. Reece,[‡] Charles M. Nichols,[‡] Steen Hammerum,[†] and Veronica M. Bierbaum*[,‡]

[†]Department of Chemistry, University of Copenhagen, Universitetsparken 5, Copenhagen, DK-2100 Denmark
[‡]Department of Chemistry and Biochemistry, University of Colorado, 215 UCB, Boulder, Colorado 80309, United States

Supporting Information

ABSTRACT: The α-effect—enhanced reactivity of nucleophiles with a lone-pair adjacent to the attacking center—was recently demonstrated for gas-phase S_N2 reactions of HOO^-, supporting an intrinsic component of the α-effect. In the present work we explore the gas-phase reactivity of microsolvated nucleophiles in order to investigate in detail how the α-effect is influenced by solvent. We compare the gas-phase reactivity of the microsolvated α-nucleophile $HOO^-(H_2O)$ to that of microsolvated normal alkoxy nucleophiles, $RO^-(H_2O)$, in reaction with CH_3Cl using a flowing afterglow-selected ion flow tube instrument. The results reveal enhanced reactivity of $HOO^-(H_2O)$ and clearly demonstrate the presence of an α-effect for the microsolvated α-nucleophile. The association of the nucleophile with a single water molecule results in a larger Brønsted β_{nuc} value than is the case for the unsolvated nucleophiles. Accordingly, the reactions of the microsolvated nucleophiles proceed through later transition states in which bond formation has progressed further. Calculations show a significant difference in solvent interaction for HOO^- relative to the normal nucleophiles at the transition states, indicating that differential solvation may well contribute to the α-effect. The reactions of the microsolvated anions with CH_3Cl can lead to formation of either the bare Cl^- anion or the $Cl^-(H_2O)$ cluster. The product distributions show preferential formation of the Cl^- anion even though the formation of $Cl^-(H_2O)$ would be favored thermodynamically. Although the structure of the $HOO^-(H_2O)$ cluster resembles $HO^-(HOOH)$, we demonstrate that HOO^- is the active nucleophile when the cluster reacts.

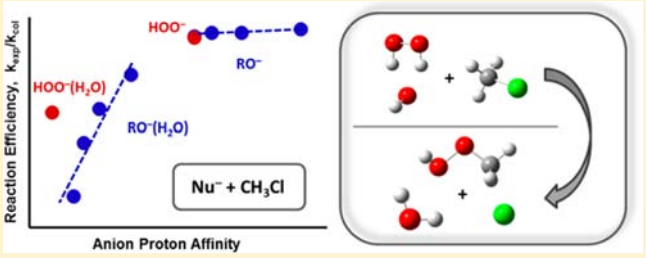

INTRODUCTION

Gas-phase ion-molecule studies provide a means to investigate the intrinsic factors that affect reactions in a solvent free environment or in an environment with a controlled number of solvent molecules, also referred to as microsolvation. Drastic differences are observed between gas-phase and condensed-phase reactivity, as rate constants of gas-phase ion-molecule reactions exceed those in solution by as much as 16 orders of magnitude.[1] Gas-phase studies of microsolvated ions are essential to provide insight into the role of the solvent in a given reaction and may shed light on the transition between gas-phase and condensed-phase reactivity.

The S_N2 reaction is a fundamental process in organic chemistry, and numerous experimental[1−11] and computational[9−15] studies have examined the reactivity of microsolvated anions in S_N2-type reactions. Nucleophilic substitution of methyl chloride is a prototypical S_N2 reaction, with no competing reaction pathways (no proton abstraction or adduct formation), and investigation of the relative nucleophilicity of different anions is straightforward, making this substrate ideal for the investigation of an α-effect for microsolvated anions.

α-Nucleophiles possess a lone pair of electrons adjacent to the attacking center, e.g. ionic nucleophiles such as the hydrogen peroxide and hypochlorite anions, or neutral nucleophiles such as hydrazine and hydroxylamine. In solution, α-nucleophiles have been shown to display enhanced nucleophilicity relative to that of normal nucleophiles of similar basicity, and the term α-effect[16] has been used to describe this deviation in reactivity relative to that expected from Brønsted-type correlations. The α-effect has been observed in several different types of reactions including S_N2 reactions.[17−23] The magnitude of the α-effect for reaction with specific substrates can be determined as the ratio of rate constants for the reactions of an α-nucleophile (k_α) and a normal nucleophile (k_{normal}) of similar basicity.[24] α-effects (k_α/k_{normal}) in the range of 5−1000 have been reported for numerous reactions in such diverse solvents as H_2O, DMSO, and CH_3CN.[25] This has led to an active controversy about whether the α-effect is controlled by inherent properties of the α-nucleophile or by external solvent effects.

Gas-phase studies provide a vital link to resolving the intrinsic nature of the α-effect. The experimental search for a gas-phase α-effect began with studies of DePuy et al.[26] who found that the hydrogen peroxide anion (HOO^-) does not show enhanced reactivity relative to hydroxide (HO^-) in reactions with methyl formate. The authors concluded that a gas-phase α-effect could

Received: July 1, 2013
Published: September 18, 2013

   dx.doi.org/10.1021/ja4066943 | J. Am. Chem. Soc. 2013, 135, 15508−15514

not be observed. This was subsequently questioned, since the gas-phase basicity of HO^- far exceeds that of HOO^-, and similar behavior would imply enhanced reactivity of the α-nucleophile.[27] Also, increased single-electron-transfer in the HOO^- transition state led Patterson and Fountain[27] to support the existence of an α-effect. However, an experimental study of the gas-phase reactivity of the α-nucleophiles HOO^-, ClO^-, and BrO^- with a comprehensive series of oxygen-centered normal nucleophiles in S_N2 reactions with methyl chloride revealed no gas-phase α-effect.[28] It was recognized that the high exothermicity of these reactions might obscure the properties of the intrinsic barriers. Subsequent studies of similar S_N2 reactions with reduced reaction exothermicity definitively showed reactivity enhancements by factors of 2.3−50 when comparing HOO^- to the normal nucleophiles HO^-, methoxide (CH_3O^-), ethoxide ($C_2H_5O^-$), and 2-propoxide (i-$C_3H_7O^-$) in reactions with methyl fluoride, anisole, and fluoroanisole.[29] These results demonstrate the existence of an intrinsic component of the α-effect. Recent studies clearly also show the presence of an α-effect in addition-elimination reactions on carbonyl carbon.[30] In addition, McAnoy et al.[31] report a gas-phase α-effect when comparing the reactions of HOO^- and CH_3O^- with dimethyl methylphosphonate, based on major differences in the product branching ratios for the two ions.

Recent theoretical studies support the premise that the α-effect has a component that can be attributed to intrinsic properties of the nucleophile.[27,32−37] Ren and Yamataka[34−37] investigated the reactivity of the α-nucleophiles, HOO^-, ClO^-, and BrO^-, with a series of alkyl chlorides by calculating the reaction barrier heights using the composite G2(+) method and comparing the results to those for normal nucleophiles. While the normal nucleophiles display a linear correlation between anion basicity and reaction barrier height, reactions of the α-nucleophiles appear to have lower barriers than predicted by this linear basicity-barrier relation, supporting an intrinsic component of the α-effect.

The α-nucleophile investigated in this study is the microsolvated hydrogen peroxide anion, $HOO^-(H_2O)$. The structure of this cluster ion has been mentioned briefly by Anick[38] in a comprehensive computational study on the incremental solvation of the HOO^- anion. However, to the best of our knowledge this is the first experimental study of the gas-phase reactivity of the α-nucleophile $HOO^-(H_2O)$. We report overall rate constants and reaction efficiencies along with product distributions for the reactions of HOO^-, HO^-, CH_3O^-, $C_2H_5O^-$, and i-$C_3H_7O^-$ with methyl chloride in the presence of a single water molecule. We investigate the α-nucleophilicity of $HOO^-(H_2O)$ by comparing the reaction efficiency to that of the microsolvated normal nucleophiles. The absence of an α-effect for HOO^- in previous gas-phase studies of nonsolvated anions with methyl chloride was ascribed to the large reaction efficiency. Incremental microsolvation has previously been shown to significantly decrease the reaction efficiency,[1−6] and we exploit the lower reactivity of the microsolvated anions to investigate the presence of an α-effect in S_N2 reactions with methyl chloride.

EXPERIMENTAL SECTION

The experiments were carried out with a flowing afterglow selected-ion flow tube (FA-SIFT) mass spectrometer at the University of Colorado, Boulder. Details of the instrument and methods have been presented elsewhere.[39,40] Briefly, the instrument consists of the following four sections: an ion-source flow tube, an ion-selection region, a reaction flow tube, and a detection region. The ions are produced in a flowing afterglow ion source and are mass selected using a quadropole mass filter prior to injection into the reaction flow tube. HO^- was prepared by electron ionization (70 eV) of methane and nitrous oxide (2:1 ratio) in helium buffer gas. HOO^- was prepared by proton abstraction from H_2O_2 by NH_2^-, which was prepared by electron ionization of NH_3. All other anions were generated by proton abstraction of the corresponding neutrals by HO^-. The microsolvated ions were prepared by introducing a mixture of H_2O in tetrahydrofuran slightly downstream of the production of bare ions. In previous studies, tetrahydrofuran was shown to enhance the formation of microsolvated ions.[41] Upon injection of the mass-selected ions into the reaction flow tube the ions are entrained in a flow of helium (~0.5 Torr), which assures a thermal energy distribution of the reactant ions prior to reaction with the neutral reagent. A known flow of neutral reagent is added through a series of equidistant inlets along the reaction flow tube, and finally ionic reagents and products are analyzed in the detection region using a quadrupole mass filter coupled to an electron multiplier.

The decrease in reactant ion signal is monitored as a function of reaction distance (which is directly correlated to the reaction time), and a rate constant is derived by assuming pseudo-first-order kinetics (reactant ion ~10^5 ions cm^{-3}, neutral reagent ~10^{11} molecules cm^{-3}). All reported reaction rate constants and product distributions represent the average of at least three individual measurements. Reaction efficiencies are the ratio between the experimental rate constant (k_{exp}) and the collision rate constant (k_{col}). Collision rate constants are calculated from parametrized trajectory collision rate theory.[42] Product distributions are determined by extrapolating the product yields to zero reaction time in order to exclude any secondary reaction products. The product distributions were corrected for reactions of the bare ion, which was always present as a result of collision-induced dissociation upon injection of the microsolvated ion into the reaction flow tube. Mass discrimination was minimized, and no corrections were applied to the data. Absolute uncertainties with respect to the rate constants are ±30%, and with respect to the product distributions they are ±50% due to uncertainties in pressure, flow, and temperature. All reagents were obtained from commercial sources and are used without further purification: methyl chloride (CH_3Cl, Matheson, 99.5%); hydrogen peroxide (H_2O_2, Sigma-Aldrich, 50 wt % solution in water); methanol (CH_3OH, Honeywell B&J, 99.9%); ethanol (C_2H_5OH, Decon Laboratories, 200 proof); isopropanol (i-C_3H_7OH, Fisher Scientific, 99.9%), tetrahydrofuran (THF, Sigma Aldrich, 99.9%), ammonia (NH_3, Airgas, 99.9995%). Helium buffer gas (He, Airgas, 99.995%) was purified by passage through a molecular sieve trap immersed in liquid nitrogen.

COMPUTATIONAL METHODS

Minimum and transition-state structures were localized as stationary points on the MP2/6-311++G(d,p) potential energy surface. Harmonic vibrational frequencies were obtained at the same level and used to verify the nature of the stationary points as minima and first-order saddle points, respectively. The structure of the $HOO^-(H_2O)$ cluster was further optimized using B3LYP/6-311++G(d,p), MP2/aug-cc-pVTZ, and CCSD(T)/ aug-cc-pVTZ. Thermodynamic properties were calculated using a modified version of the composite G3 method in which all geometry optimizations and harmonic vibrational frequency calculations were carried out with the 6-31+G(d) basis set instead of the default 6-31G(d). The diffuse functions were included to allow a better description of the anions. This treatment is comparable to the G2(+) method which has successfully been employed in previous studies of S_N2 reactions involving anions.[36,43] All MP2, B3LYP and composite calculations were carried out with the *Gaussian* 09 program.[44] CCSD(T) calculations were carried out with *Molpro* 2010.1.[45]

Proton affinities (PA) of the microsolvated nucleophiles correspond to the calculated reaction enthalpies at 298 K for the reaction:

$$Nu^-(H_2O) + H^+ \rightarrow NuH(H_2O) \quad (1)$$

dx.doi.org/10.1021/ja4066943 | J. Am. Chem. Soc. 2013, 135, 15508−15514

Table 1. Thermodynamic data, kinetic data, and product distributions for the S_N2 reactions of microsolvated anions with methyl chloride: $Nu^-(H_2O)$ + CH_3Cl

	thermodynamic data[a]			kinetic data[b]		product distribution[c]	
	PA	ΔH_{hydr}	ΔH_r	k_{exp} ($\times 10^{-11}$)	Eff	Cl^-	$Cl^-(H_2O)$
$HO^-(H_2O)$	1538	−112	−101/−161	36[d]	0.15	0.85[e]	0.15[e]
$CH_3O^-(H_2O)$	1520	−99	−103/−164	10 ± 1	0.049	0.78	0.22
$C_2H_5O^-(H_2O)$	1511	−92	−95/−155	3.3 ± 0.1	0.016	0.47	0.53
i-$C_3H_7O^-(H_2O)$	1505	−89	−82/−143	0.54 ± 0.05	0.0028	0.42	0.58
$HOO^-(H_2O)$	1493	−106	−80/−140	9.3 ± 0.3	0.044	0.72	0.28

[a]Thermodynamic data in units of kJ/mol calculated using G3; proton affinities (PA) of the microsolvated anions; hydration enthalpy (ΔH_{hydr}); reaction enthalpies (ΔH_r) displayed for Cl^- and clustered $Cl^-(H_2O)$ products respectively ($Cl^-/Cl^-(H_2O)$). [b]Overall rate constant (k_{exp}) in units of cm^3 $molecule^{-1}$ s^{-1}. Error bars represent one standard deviation, absolute uncertainty is ±30%. Reaction efficiency (Eff) is the ratio of the overall experimental rate constant (k_{exp}) to the collision rate constant (k_{col}) calculated using parametrized trajectory collision theory.[42] [c]Product distributions are determined by extrapolating the product yields to zero reaction time; absolute uncertainty is estimated as ±50%. [d]Rate constant for $DO^-(D_2O)$ + CH_3Cl obtained from ref 46; standard deviation not reported; deuteration was used to distinguish the reactant and product ion masses. [e]Product distribution is obtained from ref 3.

RESULTS AND DISCUSSION

Reaction Efficiencies. The measured rate constants and reaction efficiencies for the S_N2 reactions of microsolvated anions with methyl chloride are displayed in Table 1, together with calculated reaction thermodynamics and proton affinities of the microsolvated nucleophiles. Since the reaction with methyl chloride proceeds exclusively by an S_N2 process, the overall efficiencies can be compared directly; there is no loss of reactant from competing reaction pathways to take into account. Figure 1 shows a Brønsted-type plot of the reaction efficiency versus the proton affinity of the microsolvated anions. Efficiencies for reactions of unsolvated nucleophiles are included for comparison. The result is clear: the reaction efficiency of $HOO^-(H_2O)$ reacting with methyl chloride is more than an order of magnitude larger than would be expected from the rate-energy relationship found for the normal microsolvated nucleophiles. The microsolvated hydrogen peroxide anion definitively shows an α-effect in the S_N2 reaction with methyl chloride.

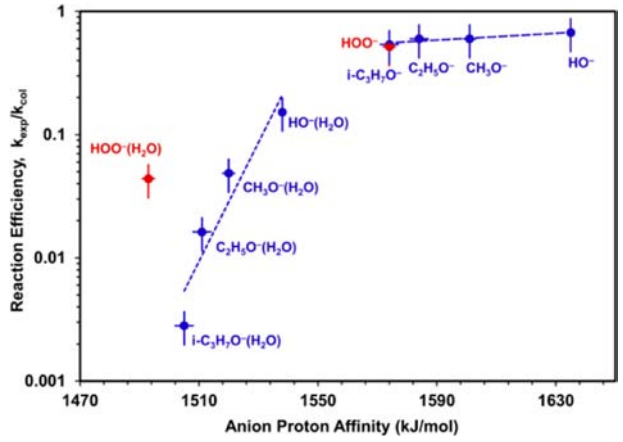

Figure 1. Reaction efficiency (k_{exp}/k_{col}) vs anion proton affinity (PA) for the S_N2 reactions of unsolvated and microsolvated anions with methyl chloride. Normal nucleophiles are displayed in blue, and α-nucleophiles, in red. The linear trend lines are fits to the normal nucleophile data sets. The reaction efficiency is the ratio of the overall experimental rate constant (k_{exp}) to the collision rate constant (k_{col}), calculated using parametrized trajectory collision theory.[42] Reaction efficiencies for the unsolvated anions are obtained from ref 28. The anion PAs are calculated using G3. The vertical error bars represent the absolute uncertainty of ±30%. The horizontal error bars represent the experimental uncertainty in the PA of the bare ion, against which the computed PAs are benchmarked.

When comparing the reaction efficiencies of the microsolvated nucleophiles with the reaction efficiencies previously reported for the corresponding nonsolvated nucleophiles[28] (Table 2), it is evident that the association of just a single water molecule has a drastic effect on the reactivity. The reaction efficiencies of the nonsolvated nucleophiles are all large and quite similar (between 0.67 and 0.52) despite a proton affinity range of more than 55 kJ/mol. In contrast, the reaction efficiencies of the microsolvated nucleophiles vary by a factor of 50 (from 0.15 for $HO^-(H_2O)$ to 0.003 for i-$C_3H_7O^-(H_2O)$), despite a smaller proton affinity span.

Table 2. Thermodynamic Data, Reaction Efficiencies and Calculated Bond Lengths for the Transition States of the S_N2 Reaction of Unsolvated Anions with Methyl Chloride: Nu^- + CH_3Cl

	PA[a]	ΔH_r[a]	Eff[b]	R_{Nu-C}[c]	R_{C-Cl}[c]
HO^-	1635 (1633)	−214	0.67	2.158	2.090
CH_3O^-	1601 (1598)	−202	0.60	2.127	2.069
$C_2H_5O^-$	1584 (1585)	−187	0.60	2.109	2.088
i-$C_3H_7O^-$	1574 (1576)	−171	0.54	2.084	2.109
HOO^-	1574 (1575)	−186	0.52	2.115	2.076

[a]Thermodynamic data in units of kJ/mol calculated using G3; calculated proton affinities (PA) of the anions with experimental values in parentheses;[47] calculated reaction enthalpies (ΔH_r) displayed for Cl^- product formation. [b]Reaction efficiency (Eff) is the ratio of the overall experimental rate constant (k_{exp}) to the collision rate constant (k_{col}) calculated using parametrized trajectory collision theory;[42] reaction efficiencies are obtained from ref 28. [c]Geometries are optimized at the MP2/6-311++G(d,p) level of theory; transition state-bond lengths (R_{Nu-C} and R_{C-Cl}) in units of Å.

Incremental microsolvation has previously been shown to significantly decrease the reaction efficiency,[1−6] and indeed, associating the nucleophile with even a single water molecule lowers the reaction efficiency and results in large reactivity differences across the series of nucleophiles; thus, the presence of an α-effect is revealed, which was not apparent for reactions of the unsolvated nucleophiles.

Product Distributions. While gas-phase S_N2 reactions of unsolvated nucleophiles with methyl chloride produce only the bare Cl^- ion, reactions of microsolvated nucleophiles have an

dx.doi.org/10.1021/ja4066943 | J. Am. Chem. Soc. 2013, 135, 15508−15514

additional product channel in which the solvated $Cl^-(H_2O)$ ion is formed:

$$Nu^-(H_2O) + CH_3Cl \rightarrow NuCH_3 + Cl^- + H_2O \quad (2a)$$

$$\rightarrow NuCH_3 + Cl^-(H_2O) \quad (2b)$$

The product distributions for formation of Cl^- and $Cl^-(H_2O)$ for the series of microsolvated nucleophiles are shown in Table 1. The microsolvated product ion is formed in the more exothermic process and this channel could well be expected to be dominant. Nonetheless, unsolvated Cl^- is the main product of the reaction of the microsolvated HOO^-, HO^-, and CH_3O^- ions with methyl chloride, and reactions of the microsolvated $C_2H_5O^-$ and i-$C_3H_7O^-$ ions form approximately equal amounts of the solvated and nonsolvated Cl^-.

Previous investigations of S_N2 reactions involving microsolvated nucleophiles and methyl chloride have shown similar product distributions in which formation of the nonsolvated product dominates.[3,4] We find that the relative yield of solvated product, $Cl^-(H_2O)$, tends to increase with increasing size of the nucleophile and with decreasing reaction exothermicity. Several factors may contribute to the preferred formation of the thermodynamically less favorable nonsolvated product; explanations suggesting steric properties,[8] product dynamics in a postreaction complex,[10] as well as redistribution of excess reaction energy[48] have been proposed. In the present study we obtain a similar product distribution for the microsolvated α-nucleophile, $HOO^-(H_2O)$, as that found for the microsolvated normal nucleophiles, which leads us to conclude that the enhanced reactivity of $HOO^-(H_2O)$ is not reflected in differences in the product distribution.

Water Cluster Structures. Representative calculated structures of the microsolvated anions are shown in Figure 2.

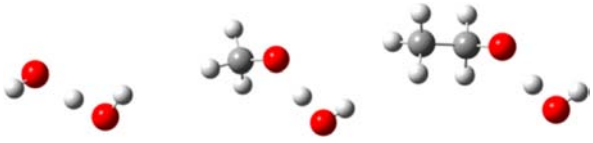

Figure 2. Lowest-energy structures of the microsolvated anions $HO^-(H_2O)$, $CH_3O^-(H_2O)$, and $CH_3CH_2O^-(H_2O)$ optimized at the MP2/6-311++G(d,p) level of theory.

All normal-nucleophiles form clusters in which the water molecule has one hydrogen oriented toward the anionic center. The computed hydration enthalpy (ΔH_{hydr}) is obtained as the enthalpy difference between the water cluster and the isolated species (Table 1). The magnitude of ΔH_{hydr} varies in the series of normal nucleophiles from −112 kJ/mol for $HO^-(H_2O)$ to −89 kJ/mol for i-$C_3H_7O^-(H_2O)$ tracking the decreasing proton affinity for the isolated anions.

Compared to the normal nucleophiles, the $HOO^-(H_2O)$ cluster has a high ΔH_{hydr} of −106 kJ/mol, even though the proton affinity of the HOO^- anion is similar to that of the i-$C_3H_7O^-$ anion. The optimized structure of microsolvated HOO^- is displayed in Figure 3 along with geometrical parameters. The $HOO^-(H_2O)$ cluster is distinctly different from the water cluster of the normal anions in that it appears to resemble $HO^-(HOOH)$, in which the HOOH behaves as a bidentate hydrogen donor toward HO^-. The structure is almost symmetrical, with nearly identical hydrogen bond lengths and hydrogen bond angles. The most conspicuous geometrical feature is the structure of the HOOH moiety, which is

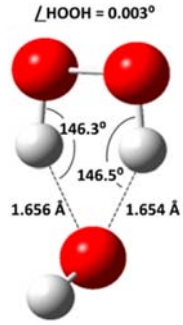

Figure 3. Lowest-energy structure of the microsolvated anion $HOO^-(H_2O)$ optimized at the CCSD(T)/aug-cc-pVTZ level of theory.

completely planar, whereas isolated hydrogen peroxide possesses a staggered conformation. This structure is even more remarkable considering that the proton affinity of HO^- (1633 kJ/mol)[47] is higher than that of HOO^- (1575 kJ/mol).[47]

This peculiar structure of the microsolvated HOO^- has been addressed briefly by Anick[38] in a comprehensive computational study on the incremental solvation of the HOO^- anion. In agreement with his results we find that two minima can be found when the structure is optimized with B3LYP/6-311++G(d,p), one corresponding to a $HOO^-(H_2O)$ structure and one corresponding to a $HO^-(HOOH)$ structure. The two isomers are separated by only a small barrier of 7 kJ/mol. When MP2/6-311++G(d,p), MP2/aug-cc-pVTZ or CCSD(T)/aug-cc-pVTZ is employed only the $HO^-(HOOH)$ structure represents a stationary point.

It is pertinent to consider whether the reactive nucleophile should be described as HOO^- solvated by a water molecule or as HO^- solvated by hydrogen peroxide. In the experiment the reactant ion is selected solely on the basis of mass, which does not distinguish between the two structures. Upon injection of the cluster into the reaction flow tube collision-induced dissociation results only in the formation of the bare HOO^-; no HO^- is observed (Figure 4). Accordingly, dissociation of the adduct into

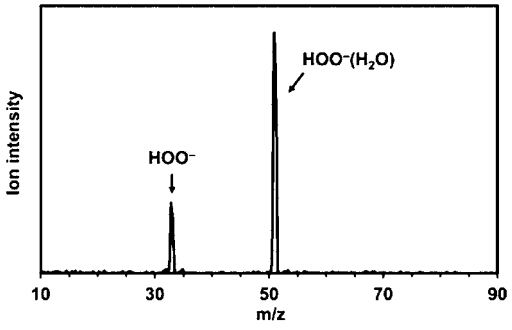

Figure 4. The mass selected spectrum of the microsolvated hydrogen peroxide anion $HOO^-(H_2O)$ (m/z 51). The bare HOO^- ion (m/z 33) was always present as a result of collision-induced dissociation upon injection of the microsolvated ion into the reaction flow tube.

HOO^- and H_2O is 60 kJ/mol more favorable than dissociation into HO^- and H_2O_2 based on experimental heats of formation for the separated species.[47] The calculated CCSD(T)/aug-cc-pVTZ energy difference between the two dissociation channels is similar (58 kJ/mol). However, this does not prove the identity of the reactive nucleophile in the cluster.

The experimental product distributions provide us with direct evidence to support the contention that HOO^- is the reactive

dx.doi.org/10.1021/ja4066943 | J. Am. Chem. Soc. 2013, 135, 15508−15514

nucleophile. It is not possible to directly demonstrate whether methyl hydrogen peroxide or methanol is formed since only the ionic products are monitored. Fortunately, the clustered ionic products differ depending on whether HOO^- or HO^- is the active nucleophile:

$$HOO^-(H_2O) + CH_3Cl \rightarrow HOOCH_3 + Cl^-(H_2O) \quad (3)$$

$$HO^-(HOOH) + CH_3Cl \rightarrow HOCH_3 + Cl^-(HOOH) \quad (4)$$

The reaction of microsolvated HOO^- with methyl chloride produces 28% $Cl^-(H_2O)$; formation of a $Cl^-(HOOH)$ product is not observed (Figure 5). This result indicates that the attacking

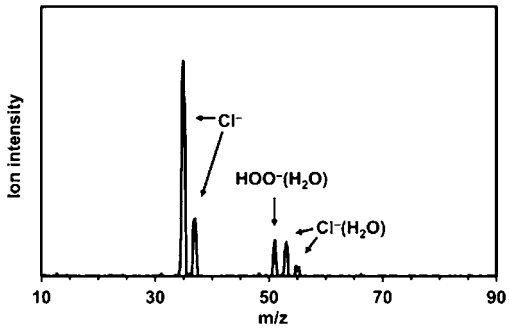

Figure 5. The product mass spectrum for the reaction between $HOO^-(H_2O)$ and CH_3Cl. Only two ionic products are detected: Cl^- at m/z 35/37 and $Cl^-(H_2O)$ at m/z 53/55. Residual reactant ion, $HOO^-(H_2O)$ is seen at m/z 51.

nucleophile is in fact HOO^-. Nevertheless, as noted by a reviewer, we cannot rigorously exclude the possibility that some of the unsolvated Cl^- is formed through a reaction in which HO^- is the reactive nucleophile. However, when the $HOO^-(H_2O)$ cluster reacts with methyl formate the products formed are solely the peroxyformate anion and clusters thereof, conclusively demonstrating that HOO^- is the only reacting nucleophile in the cluster ion.[49] Furthermore, reaction paths for reactions of $HOO^-(H_2O)$ and $HO^-(HOOH)$ with methyl chloride were examined computationally (Figure 6). The enthalpy of the transition state corresponding to $HOO^-(H_2O)$ attack is 17 kJ/mol below that of the transition state for $HO^-(HOOH)$ attack. This is consistent with the experimental results, supporting that HOO^- is the reactive nucleophile in the $HOO^-(H_2O)$ cluster. This in turn supports that the enhanced reactivity of $HOO^-(H_2O)$ can indeed be ascribed to the α-nucleophilic character of the HOO^- anion.

An intrinsic reaction coordinate (IRC) calculation was performed to investigate how the transition state corresponding to HOO^- attack connects to the $HO^-(HOOH)$ structure in Figure 3. As shown in Figure 6 (black line) the $HOO^-(H_2O)$ transition state connects to a prereaction complex in which the structure of the attacking cluster is closely related to that found in the transition state. However, in the prereaction complex we see that the hydrogen bonding OH of the water molecule is elongated, suggesting incipient proton transfer. Upon further increase of the distance between $HOO^-(H_2O)$ and CH_3Cl the proton is completely transferred from the water to the HOO^- and the attacking cluster converts into the $HO^-(HOOH)$ cluster.

Transition-State Structures. Representative calculated transition-state structures are displayed in Figure 7. In the S_N2 reactions examined the nucleophile attacks the methyl chloride opposite to the leaving chloride group, forming a trigonal

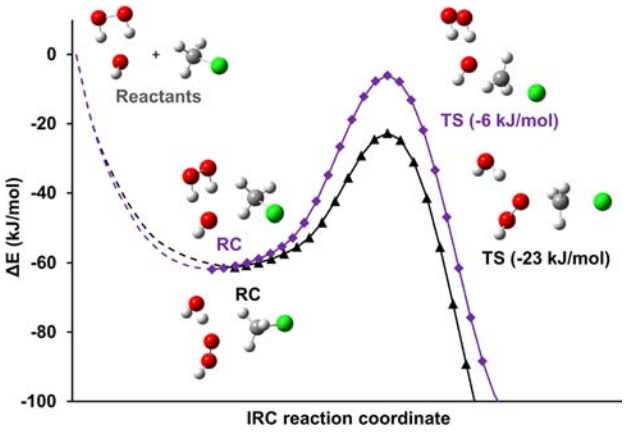

Figure 6. IRC surfaces (solid lines) for reaction of the microsolvated hydrogen peroxide anion with methyl chloride calculated using MP2/6-311++G(d,p). The black surface corresponds to HOO^- attack, the purple surface corresponds to HO^- attack. The dotted line only serves to illustrate a connection to the reactants. The structures represent MP2/6-311++G(d,p) optimized transition states (TS), prereaction complexes (RC) and reactants. In parentheses are the transition state enthalpies calculated using G3.

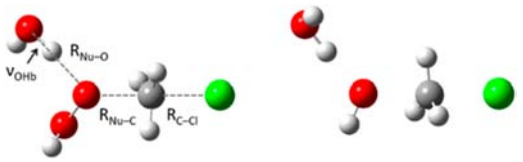

Figure 7. Transition-state structures for the S_N2 reaction of the microsolvated anions $HOO^-(H_2O)$ and $HO^-(H_2O)$ with methyl chloride optimized at the MP2/6-311++G(d,p) level of theory. The bond lengths R_{Nu-C}, R_{C-Cl}, and R_{Nu-O}, and the vibrational frequencies of the hydrogen-bonded OH stretch, ν_{OHb}, are found in Table 3 for all anions.

bipyramidal transition state. Throughout the reaction the water molecule retains one hydrogen pointing toward the nucleophilic center. The distances between the nucleophile and the carbon center (R_{Nu-C}) and between the leaving group Cl^- and the carbon center (R_{C-Cl}) are displayed in Table 3. The transition-state bond lengths vary only little between the different

Table 3. Calculated Bond Lengths, Vibrational OH_b Stretching Frequencies and OH_b Red Shifts for the Transition State of the S_N2 Reaction of Microsolvated Anions with Methyl Chloride: $Nu^-(H_2O) + CH_3Cl$

	R_{Nu-C} [a]	R_{C-Cl} [a]	R_{Nu-O} [a]	ν_{OHb} [b]	$\Delta\nu_{OHb}$ [b]
$HO^-(H_2O)$	2.062	2.157	2.602	2961	991
$CH_3O^-(H_2O)$	2.044	2.133	2.593	2964	986
$C_2H_5O^-(H_2O)$	2.030	2.151	2.604	2999	947
i-$C_3H_7O^-(H_2O)$	2.026	2.157	2.617	3043	904
$HOO^-(H_2O)$	2.023	2.141	2.637	3127	820

[a]Geometries are optimized and vibrational frequencies calculated at the MP2/6-311++G(d,p) level of theory; bond lengths are in units of Å, and frequencies and red shifts are in units of cm^{-1}; R_{Nu-C}, R_{C-Cl}, R_{Nu-O}, and ν_{OHb} are indicated in Figure 7. [b]The red shifts of the bonded OH stretching frequency ($\Delta\nu_{OHb}$) are calculated relative to the frequency of the free OH stretch (ν_{OHf}) in the attached water molecule ($\Delta\nu_{OHb} = \nu_{OHf} - \nu_{OHb}$). Deuterated alkoxy groups were used in the frequency calculation to avoid coupling between the OH_b- and CH-stretches.

dx.doi.org/10.1021/ja4066943 | J. Am. Chem. Soc. 2013, 135, 15508−15514

nucleophiles, although the $HOO^-(H_2O)$ cluster has a slightly tighter transition state in which bond formation has progressed most (shortest R_{Nu-C}). The corresponding geometrical parameters for the transition states of unsolvated nucleophiles are displayed in Table 2. It appears that the presence of a single water molecule results in a later transition state with more advanced Nu−C bond formation. A direct relationship between the magnitude of the α-effect and the extent of bond formation in the transition state has previously been established for condensed-phase reactions of other systems.[21] The Brønsted β_{nuc} parameter, which is the slope of a Brønsted plot, is also known to be directly related to the extent of bond formation in the transition state. This in turn implies that the α-effect is directly related to the magnitude of the β_{nuc} value.[21] Furthermore, it has been argued that the β_{nuc} value reflects the amount of single-electron-transfer (SET) in the transition state,[50−52] and that enhanced SET character would be directly related to a larger α-effect.[27,53] The slopes of the Brønsted plot shown in Figure 1 provide qualitative β_{nuc} values for reactions of the unsolvated and microsolvated nucleophiles. Although the data for the microsolvated nucleophiles exhibit some deviation from a straight line, a qualitative comparison demonstrates that the β_{nuc} value for the microsolvated nucleophiles is significantly larger than the β_{nuc} value for the unsolvated nucleophiles. The drastic change of the β_{nuc} value upon microsolvation is in complete agreement with the experimental finding that there is no apparent α-effect for the unsolvated nucleophiles, whereas the effect strongly influences the reactions when even a single water molecule is present.

To investigate the interaction with the solvent water molecule in the transition state, the distance between the nucleophilic center and the oxygen of the water molecule (R_{Nu-O}) as well as the frequency (ν_{OHb}) and red shift ($\Delta\nu_{OHb}$) of the hydrogen-bonded OH stretch in the water molecule are displayed in Table 3. It is well established that the IR red shift can be used to assess the strength of the hydrogen bond, as a larger red shift corresponds to a stronger hydrogen bond.[54] For the normal nucleophiles the red shifts are between 1000 and 900 cm^{-1}, decreasing from $HO^-(H_2O)$ to i-$C_3H_7O^-(H_2O)$. The red shift calculated for the $HOO^-(H_2O)$ transition state ($\Delta\nu_{OHb}$ = 820 cm^{-1}) is lower, corresponding to a weaker hydrogen bond to the water molecule in the transition state. This is in accordance with the transition state of $HOO^-(H_2O)$ having a slightly longer distance to the water molecule than do the normal nucleophiles. Although the $HOO^-(H_2O)$ cluster has the second-highest hydration enthalpy (Table 1), surpassed only by that of the $HO^-(H_2O)$ cluster, it exhibits the weakest hydrogen bond to the water molecule in the transition state. This implies that the solvent interactions for the α-nucleophile differ from those of the normal nucleophiles, and indicates that, in addition to inherent properties of the α-nucleophile, differential solvation may well contribute to the α-effect.

Formation of the clustered product $Cl^-(H_2O)$ could also proceed through a transition state in which the water molecule is transferred to the leaving group, Cl^-, prior to nucleophilic displacement. However, computational studies on the S_N2 reaction of $HO^-(H_2O)$ with CH_3Cl have shown that this entails a higher reaction barrier,[12] as would be expected from the better gas-phase leaving-group ability of the Cl^- anion than of the oxygen-centered anions. Direct dynamic simulations would be valuable in providing a better understanding of the water molecule transfer during the reaction.

CONCLUSIONS

Gas-phase S_N2 reactions of microsolvated oxygen-centered anions with methyl chloride demonstrate that an α-effect influences the reactions of microsolvated HOO^- anions. To associate the anions with just a single water molecule lowers the reaction efficiency and allows observation of an α-effect, which was not apparent in the studies of the reactions of unsolvated anions. Reactions of the microsolvated anions can lead to formation of either the bare Cl^- anion or the solvated product, $Cl^-(H_2O)$. The experimental product distributions show preferential formation of the Cl^- anion despite the thermodynamic preference for formation of $Cl^-(H_2O)$. Reaction of the microsolvated α-nucleophile, $HOO^-(H_2O)$, results in a product distribution (Cl^-: $Cl^-(H_2O)$ of 72%: 28%) similar to that of the microsolvated normal nucleophiles, showing that the enhanced reactivity of $HOO^-(H_2O)$ is not reflected in differences in the product distribution.

The structure of the $HOO^-(H_2O)$ cluster was investigated computationally. This structure can adequately be described as $HO^-(HOOH)$, in which the HOOH behaves as a bidentate hydrogen donor bonded to a HO^- moiety. Despite this peculiar structure, the experimental product distribution supports that HOO^- is the reacting nucleophile within the cluster, and in turn, that the enhanced reactivity of $HOO^-(H_2O)$ is ascribed to the α-nucleophilic character of the HOO^- anion.

In comparison to the unsolvated anions, the association of the nucleophile with a single water molecule results in later transition states in which the bond formation is more progressed. This is directly related to larger Brønsted β_{nuc} values obtained from the slopes of the Brønsted plots. Accordingly, we find that the microsolvated anions display an α-effect with methyl chloride even though the unsolvated anions do not. Hydrogen-bonding interactions with the water molecule in the transition state suggest that the α-nucleophile has a much weaker interaction with the solvating water molecule in the transition state than do microsolvated normal nucleophiles.

Microsolvation with even a single water molecule provides insight into the role of solvent on the α-effect; further studies of the behavior of the α-effect with incremental solvation will contribute materially to our understanding of the transition from gas-phase to condensed-phase reactivity.

ASSOCIATED CONTENT

Supporting Information

Energies and optimized geometries of all compounds. This material is available free of charge via the Internet at http://pubs.acs.org.

AUTHOR INFORMATION

Corresponding Author

veronica.bierbaum@colorado.edu

Notes

The authors declare no competing financial interest.

ACKNOWLEDGMENTS

We dedicate this paper to the memory of Prof. Charles H. DePuy; we are grateful for his inspiration and friendship. We thank Nicholas Demarais for helpful discussions and we gratefully acknowledge NSF (CHE-1012321 and CHE-1300886) for their financial support. D.L.T. thanks the Danish Chemical Society and the Augustinus Foundation, C.M.N.

thanks the AFOSR, and J.N.R. thanks the Colorado Diversity Initiative for financial support.

REFERENCES

(1) Bohme, D. K.; Mackay, G. I. *J. Am. Chem. Soc.* **1981**, *103*, 978−979.
(2) Bohme, D. K.; Raksit, A. B. *J. Am. Chem. Soc.* **1984**, *106*, 3447−3452.
(3) Hierl, P. M.; Ahrens, A. F.; Henchman, M.; Viggiano, A. A.; Paulson, J. F.; Clary, D. C. *J. Am. Chem. Soc.* **1986**, *108*, 3142−3143.
(4) Hierl, P. M.; Paulson, J. F.; Henchman, M. J. *J. Phys. Chem.* **1995**, *99*, 15655−15661.
(5) Seeley, J. V.; Morris, R. A.; Viggiano, A. A. *J. Phys. Chem. A* **1997**, *101*, 4598−4601.
(6) Viggiano, A. A.; Arnold, S. T.; Morris, R. A.; Ahrens, A. F.; Hierl, P. M. *J. Phys. Chem.* **1996**, *100*, 14397−14402.
(7) Takashima, K.; Riveros, J. M. *Mass Spectrom. Rev.* **1998**, *17*, 409−430.
(8) Otto, R.; Brox, J.; Trippel, S.; Stei, M.; Best, T.; Wester, R. *Nat. Chem.* **2012**, *4*, 534−538.
(9) Otto, R.; Xie, J.; Brox, J.; Trippel, S.; Stei, M.; Best, T.; Siebert, M. R.; Hase, W. L.; Wester, R. *Faraday Discuss.* **2012**, *157*, 41−57.
(10) Otto, R.; Brox, J.; Trippel, S.; Stei, M.; Best, T.; Wester, R. *J. Phys. Chem. A* **2013**, *117*, 8139−8144.
(11) Chen, X.; Regan, C. K.; Craig, S. L.; Krenske, E. H.; Houk, K. N.; Jorgensen, W. L.; Brauman, J. I. *J. Am. Chem. Soc.* **2009**, *131*, 16162−16170.
(12) Ohta, K.; Morokuma, K. *J. Phys. Chem.* **1985**, *89*, 5845−5849.
(13) Hu, W. P.; Truhlar, D. G. *J. Am. Chem. Soc.* **1994**, *116*, 7797−7800.
(14) Tucker, S. C.; Truhlar, D. G. *J. Am. Chem. Soc.* **1990**, *112*, 3347−3361.
(15) Vayner, G.; Houk, K. N.; Jorgensen, W. L.; Brauman, J. I. *J. Am. Chem. Soc.* **2004**, *126*, 9054−9058.
(16) Edwards, J. O.; Pearson, R. G. *J. Am. Chem. Soc.* **1962**, *84*, 16−24.
(17) Fountain, K. R.; Patel, K. D. *J. Org. Chem.* **1997**, *62*, 4795−4797.
(18) Fountain, K. R.; Felkerson, C. J.; Driskell, J. D.; Lamp, B. D. *J. Org. Chem.* **2003**, *68*, 1810−1814.
(19) McIsaac, J. E.; Mulhause, H. A.; Behrman, E. J.; Subbaram, J.; Subbaram, L. R. *J. Org. Chem.* **1972**, *37*, 1037−1041.
(20) Dixon, J. E.; Bruice, T. C. *J. Am. Chem. Soc.* **1971**, *93*, 6592−6597.
(21) Dixon, J. E.; Bruice, T. C. *J. Am. Chem. Soc.* **1972**, *94*, 2052−2056.
(22) Gregory, M. J.; Bruice, T. C. *J. Am. Chem. Soc.* **1967**, *89*, 4400−4402.
(23) Buncel, E.; Wilson, H.; Chuaqui, C. *Bull. Soc. Chim. Belg.* **1982**, *91*, 420−420.
(24) Hoz, S.; Buncel, E. *Isr. J. Chem.* **1985**, *26*, 313−319.
(25) Buncel, E.; Um, I. H. *Tetrahedron* **2004**, *60*, 7801−7825.
(26) DePuy, C. H.; Della, E. W.; Filley, J.; Grabowski, J. J.; Bierbaum, V. M. *J. Am. Chem. Soc.* **1983**, *105*, 2481−2482.
(27) Patterson, E. V.; Fountain, K. R. *J. Org. Chem.* **2006**, *71*, 8121−8125.
(28) Villano, S. M.; Eyet, N.; Lineberger, W. C.; Bierbaum, V. M. *J. Am. Chem. Soc.* **2009**, *131*, 8227−8233.
(29) Garver, J. M.; Gronert, S.; Bierbaum, V. M. *J. Am. Chem. Soc.* **2011**, *133*, 13894−13897.
(30) Garver, J. M.; Yang, Z.; Wehres, N.; Nichols, C. M.; Worker, B. B.; Bierbaum, V. M. *Int. J. Mass Spectrom.* **2012**, *330*, 182−190.
(31) McAnoy, A. M.; Paine, M. R. L.; Blanksby, S. J. *Org. Biomol. Chem.* **2008**, *6*, 2316−2326.
(32) Fountain, K. R. *J. Phys. Org. Chem.* **2005**, *18*, 481−485.
(33) Afzal, D.; Fountain, K. R. *Can. J. Chem.* **2011**, *89*, 1343−1354.
(34) Ren, Y.; Yamataka, H. *Org. Lett.* **2006**, *8*, 119−121.
(35) Ren, Y.; Yamataka, H. *J. Org. Chem.* **2007**, *72*, 5660−5667.
(36) Ren, Y.; Yamataka, H. *Chem.—Eur. J.* **2007**, *13*, 677−682.
(37) Ren, Y.; Yamataka, H. *J. Comput. Chem.* **2009**, *30*, 358−365.
(38) Anick, D. J. *J. Phys. Chem. A* **2011**, *115*, 6327−6338.
(39) Van Doren, J. M.; Barlow, S. E.; DePuy, C. H.; Bierbaum, V. M. *Int. J. Mass Spectrom. Ion Processes* **1987**, *81*, 85−100.
(40) Bierbaum, V. M. In *Encyclopedia of Mass Spectrometry*; Gross, M. L., Caprioli, R., Eds.; Elsevier: Amsterdam, 2003; Vol. *1*, pp 98−109.
(41) Bickelhaupt, F. M.; de Koning, L. J.; Nibbering, N. M. M. *Tetrahedron* **1993**, *49*, 2077−2092.
(42) Su, T.; Chesnavich, W. J. *J. Chem. Phys.* **1982**, *76*, 5183−5185.
(43) Glukhovtsev, M. N.; Pross, A.; Radom, L. *J. Am. Chem. Soc.* **1995**, *117*, 2024−2032.
(44) Frisch, M. J., et al. *Gaussian 09*, Revision B.01; Gaussian, Inc.: Wallingford CT, 2010.
(45) Werner, H.-J. et al. *MOLPRO*, version 2010.1. A package of ab initio programs; see www.molpro.net.
(46) DePuy, C. H.; Gronert, S.; Mullin, A.; Bierbaum, V. M. *J. Am. Chem. Soc.* **1990**, *112*, 8650−8655.
(47) Bartmess, J. E. *Negative Ion Energetics Data in NIST Chemistry WebBook, NIST Standard Reference Database*, Number 69; Lindstrom, P. J., Mallard, W. G., Eds.; National Institute of Standards and Technology: Gaithersburg, MD, 20899, http://webbook.nist.gov (retrieved Nov 16, 2012).
(48) Baer, T.; Hase, W. L. In *Unimolecular Reaction Dynamics: Theory and Experiment*; Oxford University Press: New York: 1996, pp 1−448.
(49) Thomsen, D. L.; Nichols, C. M.; Reece, J. N.; Hammerum, S.; Bierbaum, V. M. *J. Am. Soc. Mass. Spectrom.* **2013**, Submitted.
(50) Pross, A.; Shaik, S. S. *J. Am. Chem. Soc.* **1981**, *103*, 3702−3709.
(51) Bordwell, F. G.; Clemens, A. H. *J. Org. Chem.* **1981**, *46*, 1035−1037.
(52) Terrier, F.; Mokhtari, M.; Goumont, W.; Halle, J. C.; Buncel, E. *Org. Biomol. Chem.* **2003**, *1*, 1757−1763.
(53) Hoz, S. *J. Org. Chem.* **1982**, *47*, 3545−3547.
(54) Jeffry, G. A. *An Introduction to Hydrogen Bonding*; Oxford University Press: New York, 1997.